Experimental benchmarking of partial shading effect on thin-film and crystalline-silicon solar photovoltaic modules

Niazi, Kamran Ali Khan; Yang, Yongheng; Spataru, Sergiu Viorel; Mutarraf, Muhammad Umair; Séra, Dezso

Published in:
36th European Photovoltaic Solar Energy Conference and Exhibition

Publication date:
2019

Document Version
Publisher's PDF, also known as Version of record

EXPERIMENTAL BENCHMARKING OF PARTIAL SHADING EFFECT ON THIN-FILM AND CRYSTALLINE-SILICON SOLAR PHOTOVOLTAIC MODULES

Kamran Ali Khan Niazi, Yongheng Yang, Sergiu Viorel Spataru, Muhammad Umair Mutarraf,
and Dezso Sera
Department of Energy Technology, Aalborg University
Pontoppidanstraede 101, Aalborg, Denmark
E-Mail: kkn@et.aau.dk, yoy@et.aau.dk, ssp@et.aau.dk, mmu@et.aau.dk, des@et.aau.dk

ABSTRACT: Partial shading affects the performance and reliability of thin-film and crystalline-silicon (c-Si) photovoltaic (PV) modules. In this paper, the thin-film and c-Si modules are experimentally benchmarked by introducing various partial shading patterns over the modules. More specifically, experiments are performed using SPI-SUN 5600 SLP-based test-rig. The benchmarking reveals that thin-film and c-Si technologies behave differently under the same shading patterns. Furthermore, thermographic images are also presented to explore the effect of partial shading on both modules.

Keywords: PV module, shading, thin film, crystalline silicon, system performance, solar architecture, electroluminescence

1 INTRODUCTION

Generation and utilization of solar photovoltaic (PV) energy have been growing continuously due to the decreasing cost of solar PV modules and increasing environmental concerns [1]. The solar PV energy applications are also increasing, e.g., in residential rooftops, streetlights, and remote telecommunication systems. The installed capacity of solar PV energy is over 500 GWp [2] according to the International Energy Agency (IEA), where the crystalline-silicon (c-Si) technology shares over 90% of the market. However, the deployment of other technologies, especially the thin-film technology [3], is also growing rapidly due to the improved performance. Nonetheless, the c-Si technology is still dominating with around 450 GWp installed capacity [4].

In practice, the performance ratio (PR) of PV systems is lower [5]. Degradation in performance normally appears in the early years and continue to increase with aging, resulting in lower PRs [6]. The performance, as well as the life of PV modules, are greatly affected by partial shading, which in turn increases the temperature of the PV modules. The high-temperature part(s) of the PV modules is known as a hotspots, which can affect the entire PV system by damaging the PV modules [7]-[10]. Therefore, numerous inspection methods have been presented in the past to inspect hotspots, where the thermography [11] is the most widely employed one [12].

The effect of partial shading is different for c-Si and thin-film PV modules due to their distinct internal structures. Typically, c-Si solar PV modules have 60-72 PV cells in series [13], as shown in Fig. 1(a). Each cell behaves as an individual DC power source. During partial shading, the output power from the series shaded PV cells is affected and lowered. The shaded cells start acting as a load and dissipate the extra power generated by the un-shaded series-connected PV cells. To limit this, bypass diodes (two or three per PV module) are connected across 20-24 series PV cells, as indicated in Fig. 1(a). The reverse voltage across the shaded cells is limited by the bypass diodes D_1, D_2, and D_3 to bring it to a safe level [14], [15].

On the other hand, thin-film PV modules have long, narrow, and rectangular cells with a two (2D) dimensional current flow structure. These cells in thin-film PV modules

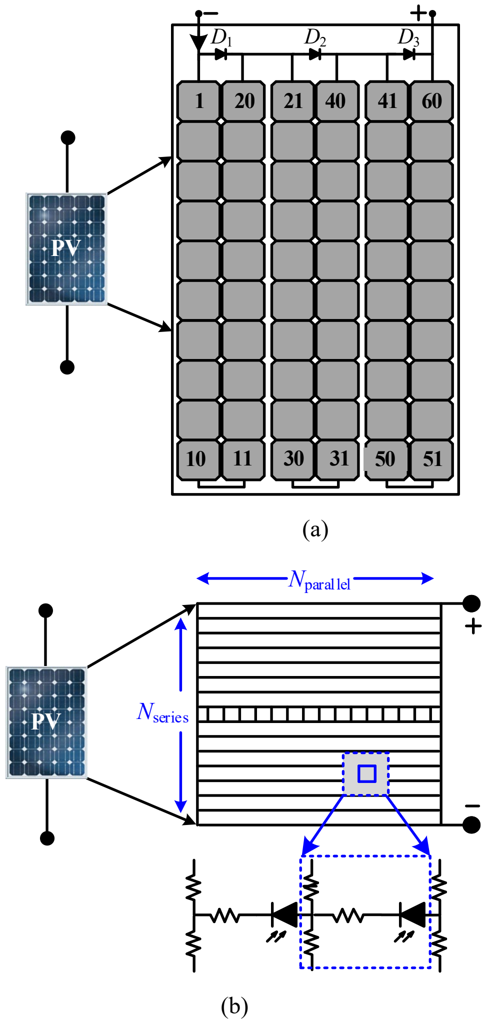

Figure 1: Internal structure of solar PV modules: (a) crystalline silicon (c-Si) and (b) thin-film.

are connected in series. The current flow is 2D in thin-film PV modules because of the internal structure, which has series-connected PV cells, as shown in Fig. 1(b) [16]. In thin-film, multiple PV sub-cells are present within each cell, which are further connected in parallel and

(a)

(b)

(c)

Figure 2: Experimental test setup: (a) SPI-SUN 5600 SLP apparatus used for experiments, (b) vertical shading on the c-Si solar PV module (SV36-150), and (c) horizontal shading on the thin-film solar PV module (SF150-S).

represented by $N_{parallel}$, as shown in Fig. 1(b).

In thin-film PV modules, the parallel-connected sub-cells depend upon the width and area of the PV module. The number of series-connected PV cells is represented as N_{series} depending on the PV module length [17], as observed in Fig. 1(b). The thin-film PV module has a completely different physical internal structure in comparison to the c-Si. Therefore, the effect of partial shading on both technologies also varies. A single bypass diode is connected across the thin-film PV module to limit the effect of shading when connected in series with other PV modules.

Experimental comparisons among thin-film and c-Si-based PV modules under various partial shading scenarios should be performed to further explore the impact. Therefore, in this paper, different partial shading cases are developed and studied experimentally by using the SPI-SUN 5600 test-rig, which is shown in Fig. 2(a). Both PV modules, i.e., the c-Si (SV36-150) in Fig. 2(b) and thin-film (SF150-S) in Fig. 2(c) are shaded vertically and horizontally to explore the effect of partial shading. The rest of this paper is arranged as follows. In Section II, the partial shading cases are described, which are used to analyze the partial shading effect on the above-mentioned PV modules. In Section III, experimental results are discussed. Finally, conclusions are drawn in Section IV.

2 PARTIAL SHADING CASES

To study the effect of partial shading on thin-film and c-Si modules, various cases (in total six cases) are developed. The first three cases are for vertical shading with different shading percentage, i.e., 33%, 66%, and 100%. Similarly, the other three cases are for horizontal shading, i.e., 33%, 66%, and 100%, as shown in Fig. 3. In Case 1, both PV modules (i.e., thin-film and c-Si) are 33% horizontally shaded by an object, as exemplified in Fig. 2(c). In Case 2 and Case 3, the PV modules are 66% and 100% shaded with the same shading object, as shown in Figs. 3(b) and (c). Similarly, for the cases from 4 to 6, a shading object (see Fig. 2(b)) shades the PV modules vertically up to 33%, 66%, and 100%, respectively, as shown in Figs. 3(d)-(f).

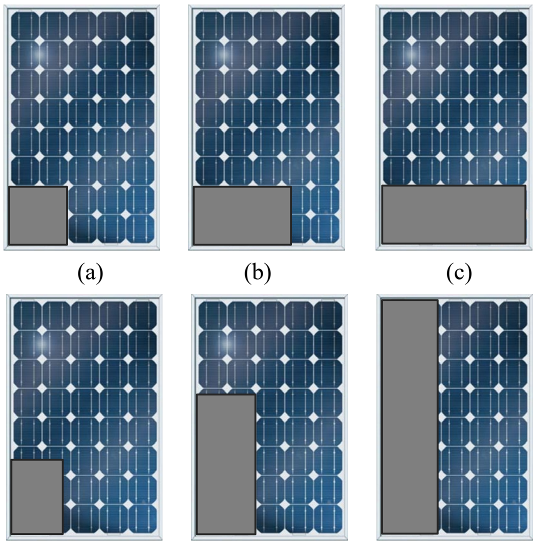

(a) (b) (c)

(d) (e) (f)

Figure 3: Partial shading cases for the thin-film and c-Si PV modules: (a) case 1: 33% horizontal shading, (b) case 2: 66% horizontal shading, (c) case 3: 100% horizontal shading, (d) case 4: 33% vertical shading, (e) case 5: 66% vertical shading, and (f) case 6: 100% vertical shading.

In order to evaluate the performance of thin-film and c-Si PV modules, experiments are performed based on the above-discussed cases. The SPI-SUN 5600 SLP apparatus is used for experimentation. A 150-Wp thin-film and 150-Wp c-Si PV modules are used in the experiments. The rating of PV modules under test is given in Table I. The performance of both PV modules under various partial shading cases are evaluated by analyzing the power-voltage (P-V) curves. The experimental results are shown in Fig. 4.

Table I: Rating of the c-Si PV module at STC

Rating	c-Si	Thin-film
Rated power	150 W	150 W
Power tolerance	+ 4.9 W	+10% / -5.0%
Short circuit current (I_{sc})	8.82 A	2.20 A
Open circuit voltage (V_{oc})	22.6 V	110.0 V
Rated current (I_{max})	8.27 A	1.88 A
Rated voltage (V_{max})	18.3 V	80.0 V

As shown in Fig. 4, the output power from both technologies is around 148 W without shading. Under various shading scenarios, PV modules behave differently, which can be seen from Fig 4. Figs. 4(a) and (b) show the

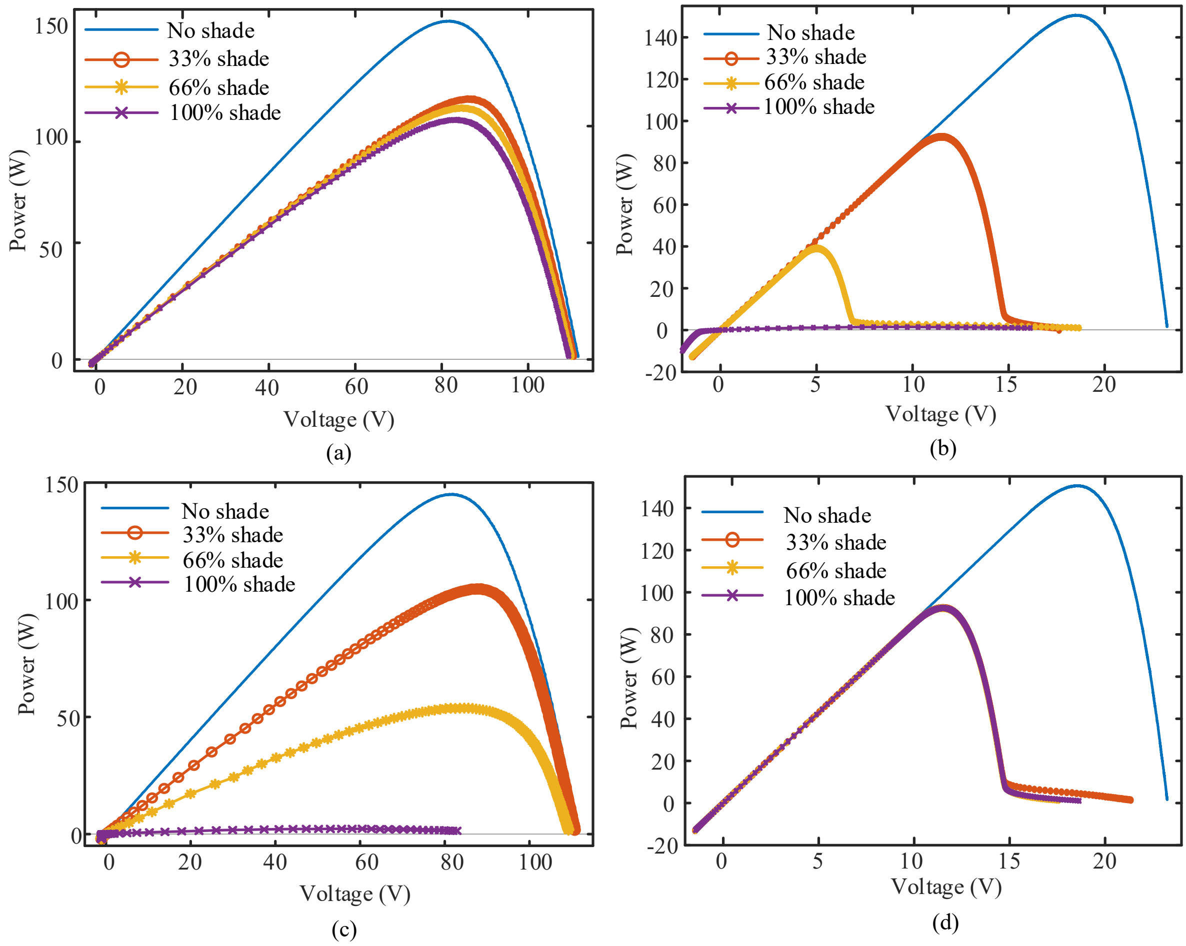

Figure 4: P-V characteristics for thin-film and c-Si PV modules under various partial shading cases: (a) horizontal shading on the thin-film PV module, (b) horizontal shading on the c-Si PV module, (c) vertical shading on the thin-film PV module, and (d) vertical shading on the c-Si PV module.

P-V characteristics under the horizontal shading on the thin-film and c-Si PV modules, respectively. In Fig. 4(a), the maximum output power obtained for the cases, i.e., Case 1, Case 2, and Case 3, is 115 W, 107.6 W, and 103.4 W, respectively. For the thin-film PV module, the output power decreases with an increase of the shading but still, it produces more than 100 W even for Case 3, where the PV module is completely (100%) horizontally shaded from the bottom. On the other hand, the c-Si module shows a significant decrease in the output power during horizontal shading, which can be seen from Fig. 4(b). More specifically, the c-Si PV module produces around 1.4 W power when it is 100% horizontally shaded, 92.6 W for Case 1, and 39.1 W for Case 2. In all, under the horizontal shading cases, the c-Si module consumes power, which increases with shading, as shown in Fig. 4(b). It is due to the placement of series cells within a c-Si PV module. The current flow is blocked by covering the area horizontally, as shown in Fig. 1(a).

For the vertical shading, the output from the thin-film PV module decreases with an increase of shading, as shown in Fig. 4(c). The output power is near to 2.2 W during 100% shading (i.e., Case 6) on the thin-film PV module. However, the output power for Case 4 and Case 5 for the thin-film PV module is 104.2 W and 53.7 W, respectively. Despite this, there is no power consumption in the thin-film module. Hence, the possibility of hotspot occurrence is not severe in the thin-film module. In the vertical shading, the c-Si still produces power even for 100% vertical shading (i.e., Case 6) because of its internal structure, which consists of bypass diodes. These bypass diodes start to operate and maintain the power from other un-shaded PV sub-modules by bypassing the shaded PV sub-module(s). Therefore, the output power for the Case 5 and Case 6 is around 92.5 W for the c-Si PV module.

To analyze the shading effect, thermography is used. A FLIR Vue 640 pro is used to capture thermal images, which are used to assess hotspots for the c-Si and thin-film PV modules, as shown in Fig. 5. During normal conditions (no-shade) in a c-Si PV module, the PV module has no hotspots, which is shown in Fig. 5(a). The consumption of power in the c-Si produces hotspots, which can be seen from the thermal images, as shown in Fig. 5. However, the hotspot occurring is not severe in thin-film PV modules due to the internal structure, as discussed previously. The temperature of the PV module during no-shade is about 49 °C at 860 W/m^2 solar irradiance. The thermal image for the c-Si PV module with a bottom left cell (cell 10 in Fig. 1(a)) is half-shaded by a thick sheet, as shown in Fig. 5(b). During this case, a bypass diode bypasses the sub-module. Hence, the sub-module (cell 1–20 in Fig. 1(a)) is now completely bypassed. Therefore, there is no contribution to the power output from this PV sub-module. The power produced by these cells is dissipated within it, which appears as a hotspot in Fig. 5(b). The hotspot temperature in Fig. 5(b) is measured around 86 °C, while the shaded

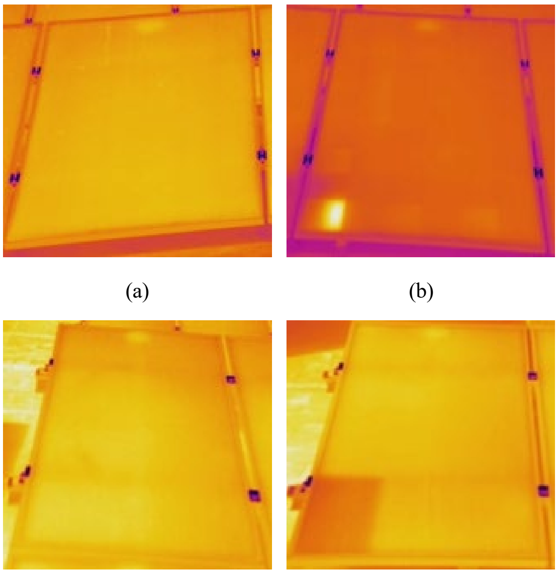

Figure 5: Thermal image of c-Si and thin-film PV modules: (a) c-Si PV module under no shade, (b) hotspot in c-Si PV module under partial shading, (c) thin-film PV module under no shade, and (b) thin-film PV module under partial shading on the bottom part of the module.

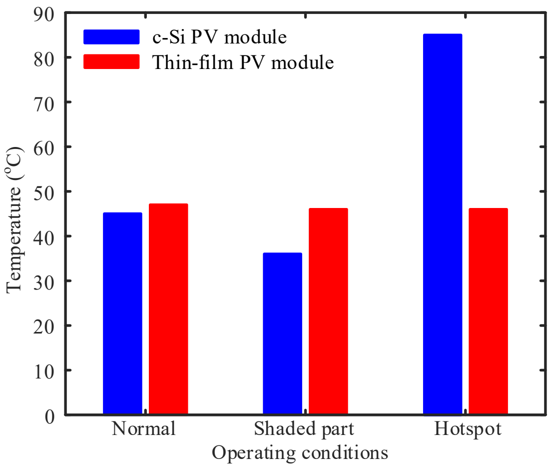

Figure 6: Effect of shading in terms of temperature on c-Si and thin-film PV modules under various conditions.

part reduces to 33 °C. The temperature of the further two un-bypass PV sub-modules remains around 49 °C, which is measured by a temperature gun.

Since, thin-film PV modules have a 2D current-flow structure, the behavior of thin-film modules is different under shading conditions. The thin-film module is also shaded by using a thick sheet. During shading, the shaded portion appears as a darker having a low temperature of 44 °C. However, the un-shaded PV sub-cell has a slightly higher temperature at 48 °C, which can be seen in Fig. 5(d). Hence, the un-shaded portion of the thin-film PV cell can contribute to the module current, since the current has multiple directions to flow.

In Fig. 6, the measured temperatures during different situations of shading for above-discussed PV modules are shown. It can be observed in Fig. 6 that in no-shade condition both c-Si and thin-film modules are working at a similar temperature. However, during shading, the temperature of the hotspots in the c-Si module is higher up to 90°, which may possibly affect the reliability of the PV modules. As the short-circuit current in c-Si PV modules is higher, the effect of hotspots during shading is severe than c-Si. Usually, the open-circuit voltages of thin-film PV modules are higher, and have lower short-circuit currents. Therefore, hotspots temperature is lower in thin-film PV modules.

3 CONCLUSIONS

In this paper, the effect of partial shading on two PV module technologies, i.e., thin-film and c-Si, was explored. Experimental results for six partial shading cases were presented in this paper. The results have shown that both technologies are affected by the designed partial shading scenarios. In all, the c-Si PV module is significantly affected due to the consumption of power produced by un-shaded series PV cells. Hence, it produces more stresses, which in-turn affects the overall life and performance of the c-Si PV module than the thin-film PV module. Moreover, experimental results based on thermography show that the occurrence of hotspots in the c-Si module is severe.

4 REFERENCES

[1] K. H. Solangi, M. R. Islam, R. Saidur, N. A. Rahim, and H. Fayaz, "A review on global solar energy policy," *Renewable and Sustainable Energy Reviews*, vol. 15, no. 4, pp. 2149–2163, May 2011.
[2] E. Kabir, P. Kumar, S. Kumar, A. A. Adelodun, and K.-H. Kim, "Solar energy: potential and future prospects," *Renewable and Sustainable Energy Reviews*, vol. 82, pp. 894–900, Feb. 2018.
[3] R. W. Birkmire, "Compound polycrystalline solar cells:: Recent progress and Y2K perspective," *Solar Energy Materials and Solar Cells*, vol. 65, no. 1, pp. 17–28, Jan. 2001.
[4] F. R. Pazheri, M. F. Othman, and N. H. Malik, "A review on global renewable electricity scenario," *Renewable and Sustainable Energy Reviews*, vol. 31, pp. 835–845, Mar. 2014.
[5] D. C. Jordan and S. R. Kurtz, "Photovoltaic degradation rates—an analytical review," *Progress in Photovoltaics: Research and Applications*, vol. 21, no. 1, pp. 12–29, Jan. 2013.
[6] P. Manganiello, M. Balato, and M. Vitelli, "A survey on mismatching and aging of PV modules: The closed loop," *IEEE Transactions on Industrial Electronics*, vol. 62, no. 11, pp. 7276–7286, Nov. 2015.
[7] A. Mellit, G. M. Tina, and S. A. Kalogirou, "Fault detection and diagnosis methods for photovoltaic systems: A review," *Renewable and Sustainable Energy Reviews*, vol. 91, pp. 1–17, Aug. 2018.
[8] S. Ahsan, K. A. K. Niazi, H. A. Khan, and Y. Yang, "Hotspots and performance evaluation of crystalline-silicon and thin-film photovoltaic modules," *Microelectronics Reliability*, vol. 88–90, pp. 1014–1018, Sep. 2018.
[9] K. Niazi, H. A. Khan, and F. Amir, "Hot-spot reduction and shade loss minimization in crystalline-silicon solar panels," *Journal of Renewable and Sustainable Energy*, vol. 10, no. 3, p. 033506, May 2018.
[10] K. A. K. Niazi, W. Akhtar, H. A. Khan, Y. Yang, and S. Athar, "Hotspot diagnosis for solar photovoltaic modules using a naive bayes classifier," *Solar Energy*, vol. 190, pp. 34–43, Sep. 2019.
[11] Y. Hu, W. Cao, J. Ma, S. J. Finney, and D. Li, "Identifying PV module mismatch faults by a thermography-based temperature distribution analysis," *IEEE Transactions on*

Device and Materials Reliability, vol. 14, no. 4, pp. 951–960, Dec. 2014.

[12] K. Niazi, W. Akhtar, H. A. Khan, S. Sohaib, and A. K. Nasir, "Binary classification of defective solar PV modules using thermography," in proc. of *2018 IEEE 7th World Conference on Photovoltaic Energy Conversion (WCPEC) (A Joint Conference of 45th IEEE PVSC, 28th PVSEC 34th EU PVSEC)*, 2018, pp. 0753–0757.

[13] M. C. Alonso-García, J. M. Ruiz, and F. Chenlo, "Experimental study of mismatch and shading effects in the I–V characteristic of a photovoltaic module," *Solar Energy Materials and Solar Cells*, vol. 90, no. 3, pp. 329–340, Feb. 2006.

[14] K. A. K. Niazi, Y. Yang, H. A. Khan, and D. Sera, "Performance benchmark of bypassing techniques for photovoltaic modules," in proc. of *2019 IEEE Applied Power Electronics Conference and Exposition (APEC)*, 2019, pp. 3164–3168.

[15] K. A. K. Niazi, Y. Yang, and D. Sera, "Review of mismatch mitigation techniques for PV modules," *IET Renewable Power Generation*, vol. 13, no. 12, pp. 2035–2050, Jun. 2019.

[16] N. D. Kaushika and A. K. Rai, "An investigation of mismatch losses in solar photovoltaic cell networks," *Energy*, vol. 32, no. 5, pp. 755–759, May 2007.

[17] S. Dongaonkar, C. Deline, and M. A. Alam, "Performance and reliability implications of two-dimensional shading in monolithic thin-film photovoltaic modules," *IEEE Journal of Photovoltaics*, vol. 3, no. 4, pp. 1367–1375, Oct. 2013.